Journal of Inorganic Biochemistry 199 (2019) 110780

Contents lists available at ScienceDirect

Journal of Inorganic Biochemistry

journal homepage: www.elsevier.com/locate/jinorgbio

Review article

Metal-based antibody drug conjugates. Potential and challenges in their application as targeted therapies in cancer

Virginia del Solar[a], María Contel[a,b,c,d,e,*]

[a] Department of Chemistry, Brooklyn College, The City University of New York, Brooklyn, NY 11210, USA
[b] Biology PhD Program, The Graduate Center, The City University of New York, 365 Fifth Avenue, New York, NY 10016, USA
[c] Biochemistry PhD Program, The Graduate Center, The City University of New York, 365 Fifth Avenue, New York, NY 10016, USA
[d] Chemistry PhD Program, The Graduate Center, The City University of New York, 365 Fifth Avenue, New York, NY 10016, USA
[e] Cancer Biology Program, University of Hawaii Cancer Center, University of Hawaii at Manoa, Honolulu, USA

ARTICLE INFO

Keywords:
Antibody drug conjugates
Metal
Cancer
Targeted therapy
Nanomedicine

ABSTRACT

Antibody drug conjugates have emerged as a very attractive type of targeted therapy in cancer. They combine the antigen-targeting specificity of monoclonal antibodies (mAbs) with the cytotoxic potency of chemotherapeutics. This review focuses on antibody drug conjugates based on metal-containing cytotoxic payloads. We will also describe antibody drug conjugates (ADCs) in which a metal-based component (mostly metallic nanoparticles) exerts a relevant function in the ADC (for photodynamic or photothermal therapy, as air-plasma-enhancer or chemo-sensitizer, as carrier of other cytotoxic payloads or as an integral part of the linker structure). Challenges and opportunities to increase the translational potential of these ADCs will be discussed.

1. Introduction

Antibody-drug conjugates (ADCs) represent a promising therapeutic approach for cancer chemotherapy with some ADC-based treatments currently available to treat blood and solid tumor cancers [1–10]. These conjugates (Fig. 1.A.) potentially combine the antigen-targeting specificity of monoclonal antibodies with the cytotoxic potency of chemotherapeutics.

Monoclonal antibodies (mAbs) are antibodies or immunoglobulins (Ig) that are produced by clones of a unique parent immune cell. These antibodies bind to the same antigenic determinant (or epitope) of an antigen through a part known as paratope. The characteristic of mAbs is their monovalent affinity for the antigen in an interaction similar to that of a lock and a key. Human tumor cells have unique or over-expressed tumor-specific antigens and mAbs can specifically bind to these antigens. Consequently, mAbs have been used as anticancer agents as they can induce an immunological response or inhibit cellular signaling pathways. However, therapeutic efficacy is limited by the cell death effect that the mAb may generate [1]. The vast majority of cytotoxic drugs do not discriminate between tumor and healthy tissues and the use of mAbs as targeting vehicles to deliver a cytotoxic payload to a tumor cell may give rise to more selective chemotherapeutic treatments [1]. There are already four ADCs currently in the clinic: Adcetris® (brentuximab vedotin) approved in 2011; Kadcyla® (Trastuzumab emtansine or T-DM1) approved in 2013, inotuzumab (Besponsa™) and *gemtuzumab ozogamicin* (Mylotarg™) both approved by the FDA in 2017. In addition, there are nearly 175 investigational ADCs in development (including around 65 compounds in clinical trials with 8 recommended "to be watched" in 2019 [11]). The United States ADC market was expected to have reached US$ 3 billion by 2018 [12].

As described by Ducry et al. [2] for ADCs to be successful, several aspects have to be considered: a) circulation and stability in plasma (behavior like a naked Ab and high stability of the linker); (b) the attachment of the cytotoxic agent does not need to disturb the antigen binding specificity; (c) efficient internalization process to achieve sufficient intracellular concentration; (d) efficient drug release of cytotoxic agent; and finally (e) high potency of the released drug (sub-nanomolar concentrations desirable although drugs with IC_{50} above that range could potentially be used if appropriate linkers employed [13]). During the past years an extraordinary amount of effort has been put into developing and improving conjugation technologies thanks to a much better understanding of the different components of the ADC. More recently, studies on processes like intramolecular trafficking [14], internalization (as not all ADCs are internalized [15]) and resistance [16] of ADCs have become very relevant for the design of optimized ADCs versions. For example, while non-internalized ADCs may be advantageous and release the payload in the tumor extracellular space affecting cells in a long residence time which might be antigen-negative, the

* Corresponding author at: Department of Chemistry, Brooklyn College, The City University of New York, Brooklyn, NY 11210, USA.
E-mail address: MariaContel@brooklyn.cuny.edu (M. Contel).

https://doi.org/10.1016/j.jinorgbio.2019.110780
Received 19 March 2019; Received in revised form 8 July 2019; Accepted 14 July 2019
Available online 18 July 2019
0162-0134/

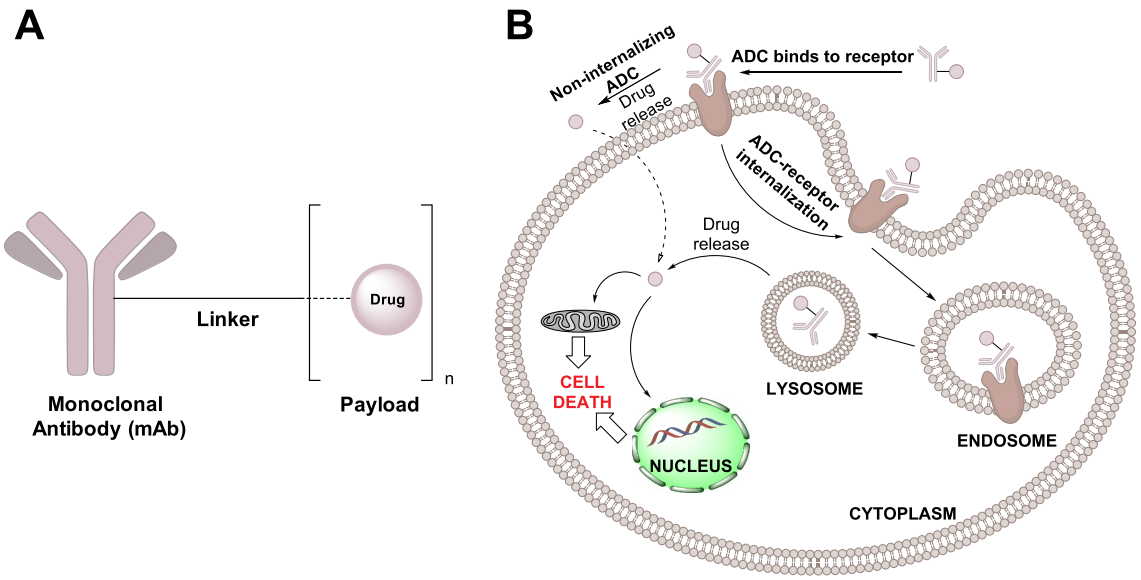

Fig. 1. A. Scheme of an antibody drug conjugate with the three main components. B. Schematic view of the mode of action of ADCs.

internalization of specific payloads (like photosensitizers) is necessary to reduce damage in the proximal tissue of targeted cells [17]. Besides, non-internalized ADCs might be of interest in molecular imaging since antibody internalization will not present a "black box" in the targeting process [17].

The current focus on ADCs is the development of a new generation of ADCs by judicious choice of the target antigen and the cytotoxic payload, by improving the properties of the linker, and by reducing drug resistance. Linkers play a tremendous role in the design of successful ADCs [1–10]. Different types of linkers have been used [1–10,18]: chemically labile, enzyme-labile, non-cleavable and most recently, linkers that are site-specific [19–22] and that have shown to eliminate heterogeneity, improve conjugate stability, and increase the therapeutic window. Most of the ADCs currently in the clinical and preclinical pipeline for cancer chemotherapy are based on complex organic molecules [1–10]. In contrast, the conjugation of metallodrugs to mAbs has been overlooked when there is enormous potential in this area with the resurgence of metal-based drugs as prospective cancer chemotherapeutics including some highly cytotoxic [23–26]. In addition, several reports have shown a positive effect (synergistic) in combination therapies based on platinum cytotoxic agents and monoclonal antibodies (both in clinical trials [27–30] and in pre-clinical studies [31–36]). Metal-based ADCs could also offset the high cost-of-goods in the preparation of these targeted chemotherapeutics as their bioconjugation to mAbs can be less complex than that of the cytotoxic payloads based on organic molecules and natural products.

This review focuses on antibody drug conjugates based on metal-containing cytotoxic payloads reported until February of 2019 [37–51]. In addition, we will briefly describe antibody drug conjugates in which a metal-based component (mostly metallic nanoparticles) exerts a relevant function in the ADCs (for photodynamic [52–54] or photothermal therapy [55–61], as chemo-sensitizer [62,63], as carrier of other cytotoxic payloads [64–66] or as an integral part of the linker structure [67–70]). This review will not include antibody-radionuclide conjugates (ARCs) for which the ADC approach is used to radiolabel antibodies that target specific tumors (theranostic agents). A number of excellent reviews on this topic have been reported recently [71–73].

2. ADCs containing metal-based cytotoxic payloads

As mentioned in the Introduction, the number of antibody drug conjugates containing a metal-based cytotoxic payload is still limited with most reports based on platinum compounds [37–49] and two very recent reports [50,51] focused on gold complexes which we will describe in the next sub-sections.

2.1. ADCs containing platinum-based payloads

2.1.1. Platinum compounds directly conjugated to mAbs

The conjugation of platinum-based drugs to antitumor antibodies (named Pt-Ig conjugates at the time) was reported as early as 1982 by Wilchek and co-workers [37]. Similar complexes of platinum and antibodies had been previously described for use in crystallographic studies [74]. Platinum salts like K_2PtCl_4 and cisplatin (*cis*-DDP) depicted in Fig. 2, were directly incubated with different inmunoglobulin Ig antibodies (including some tumor cell-reactive) such as NGIg, anti-YAC Ig, goat anti-38C13Ig, mouse anti-YAC monoclonal Ig, and human serum albumin (HAS) for 2–3 h in buffer (pH below 7.0) by an optimized method and the amount of Pt determined [37]. The authors demonstrated that the antigen binding capacity of the antitumor Ab was almost fully retained [37]. The authors also reported that the Pt-Ig complexes with specificity towards a particular mice tumor cell, were able to inhibit DNA synthesis by that cell more efficiently than the platinum compounds conjugated to non-tumor reactive antibodies or to platinum conjugated to HSA or the platinum compounds themselves [37].

Years later in 1990, Rosenblum and co-workers reported on the use of a platinum-specific antibody to conjugate the platinum(II) compound methyliminodiacetato-*trans*-*R*,*R*-1,2-diamminocyclohexane (MIDP in Fig. 2) [38]. This study was based on previous results by this group that had shown that prior adsorption to monoclonal antibodies specific to biological response modifiers (such as interferon and radioisotopes) can substantially modify their pharmacological profile (mainly their plasma pharmacokinetics and tissue distribution). The authors developed a murine monoclonal antibody (designated as 1C1) and demonstrated its preferential binding to the 1,2-diamminocyclohexane (DACH in Fig. 2) side-chain of the MIDP platinum complex at low concentrations [38]. The antibody-Pt conjugate 1C1-MIDP shows similar cytotoxicity to free Pt derivative MIDP in MCF-7 breast cancer cells. Moreover, the selective alteration of the *in vivo* pharmacology by the 1C1-MIDP conjugate with respect to MIDP was demonstrated. Pharmacokinetic studies using a labeled MIDP analogue ($[H^3]$-MIDP) and 1C1-MIDP showed considerably longer lives of the antibody-MIDP conjugate and a lower overall clearance rate in plasma. In addition, the 1C1 antibody

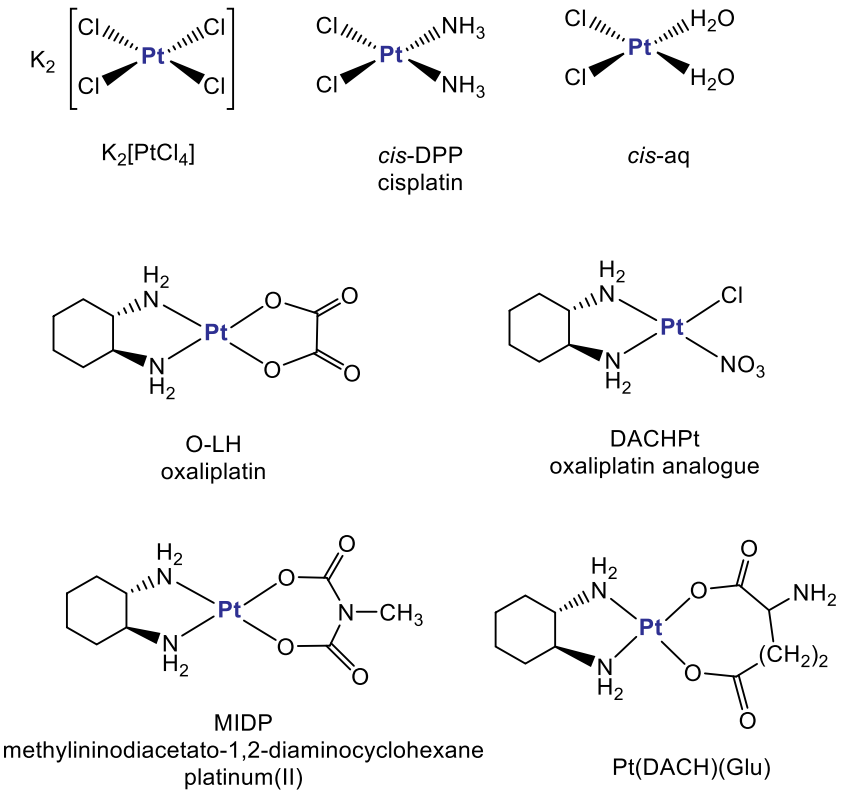

Fig. 2. Different platinum compounds used as cytotoxic payloads and conjugated to or encapsulated in delivery vehicles conjugated to antibodies.

prevented MIDP distribution to most organs and decreased dramatically its concentration in intestine, liver, kidney, and skeletal muscle. The results gave rise to a US patent issued in 1991 [39].

2.1.2. Platinum compounds conjugated to mAbs via carriers or linkers

There is a disadvantage notwithstanding in generating platinum compounds directly bound to antibodies. Antibodies do not bind significant amounts of releasable platinum (II) and the conjugates tend to be insoluble and precipitate even at low ratios of platinum (II) compounds or salts to Ab. The conjugation of platinum (II) compounds to Abs can be achieved by employing water soluble carriers [40–42]. It is important that the conjugates formed are able to dissociate from the carrier to release the platinum(II) drug so moderate to low stability is key [41,42]. It is also relevant to control the molecular size of the conjugates for a better response *in vivo* (distribution in tissues and clearance) [41,42].

2.1.2.1. Conjugates containing carboxylmethyl dextran (CM-dex) as carrier. Platinum (II) compounds (including those of pharmacological interest) are known to form reversible complexes with carboxyl groups on macromolecules [75–77]. The reversibility of the stability of these bonds depends on the polymeric structure of the macromolecule. This property was exploited by Schechter and co-workers to bind platinum (II) complexes such as *cis*-DDP and *cis*-aq (Fig. 2) to carboxymethyl dextran (CM-dex in Scheme 1) to generate complexes that are stable in aqueous solution at 4 °C for at least three weeks [75]. CM-dex complexes of these platinum(II) compounds are pharmacologically active both *in vitro* and *in vivo*. The binding of the platinum(II) compound to the polycarboxylate does not affect much the activity with respect to the free drugs [76,77].

In 1987, Schechter and co-workers reported on the modification of CM-dex (derived from Dextran T40) with idiotopic antibodies that recognize a specific membrane IgM on the B lymphoma cells (CM-dex-Ig) and the subsequent conjugation to *cis*-DDP and *cis*-aq complexes (Scheme 1) [40]. The CM-dex-Ig platform (that can be obtained pure and is highly soluble in water) is mixed in double distilled water with the platinum compounds at 37 °C for 6 h and the final conjugates can be purified by dialysis. The new specific Pt-CM-dex-Ig compounds (Pt-CM-dex-g-anti-38C-13) carried 50 mol drug/mol Ig and maintained most of the original cell-binding activity of the antibodies [40]. The specific complexes were significantly more effective against tumor 38C-13 cells (a murine model of a B lymphoma cell) than the free platinum drugs or the drugs bound to CM-dex at concentrations below 20 μM (incubation time 1–2 h). Above this range, the free drugs were more effective most plausibly due to an increased uptake in the cells [40].

An identical strategy was reported by Rowland and co-workers in 1994 to conjugate *cis*-DDP to an anti-CEA (carcinoembryonic antigen) monoclonal antibody (A5B7) *via* a CM-dex linker [41]. Conjugate A5B7-CM-dex-*cis*-DDP retained the ability to bind to CEA expressed on the surface of LS174T colorectal carcinoma cells. The authors also conjugated non-specific antibodies 1E1 and 27.8.1 to CM-dex which were subsequently bound to *cis*-DDP to generate non-specific Ab-CM-dex-*cis*-DDP for comparison purposes. The toxicity *in vitro* for the specific and non-specific Ab-CM-dex-*cis*-DDP, for CM-dex-*cis*-DDP and native or "free" *cis*-DDP was investigated on LS174T colorectal carcinoma cells. After 24 h incubation the cytotoxicity of the selective conjugate was slightly lower than that of *cis*-DDP (3 μM *versus* 7 μM) [41].

Studies *in vivo* (LS174T tumor-bearing nude mice) showed that the specific conjugate A5B7-CM-dex-*cis*-DDP (single intravenous bolus administration of a *cis*-DDP equivalent of 5 mg/kg) is more efficient than native *cis*-DDP [42]. The authors claimed that this was due to the maintenance of higher *cis*-DDP concentrations at the tumor site for A5B7-CM-dex-*cis*-DDP and a lower clearance of the specific Ab conjugate with respect to *cis*-DDP [42]. This effect was nevertheless lost at higher platinum concentrations (10 mg/kg) [41]. The pharmacokinetics and tissue distribution of the conjugate A5B7-CM-dex-*cis*-DDP were studied in CD1 mice and compared to that of free *cis*-DDP and CM-dex-*cis*-DDP [42]. The platinum (II) drug clearance rate is reduced when

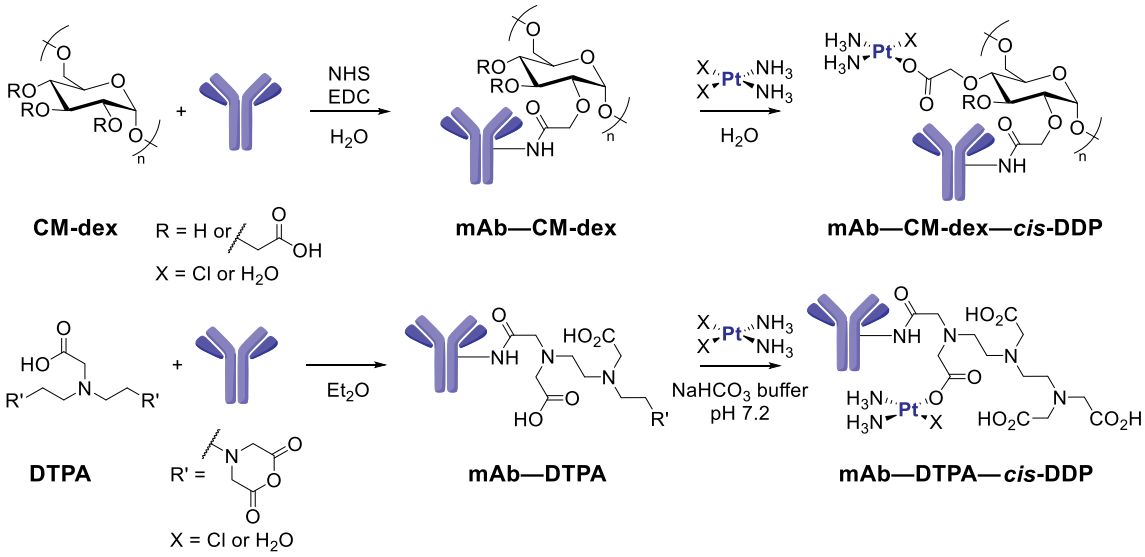

Scheme 1. Structures of carboxymethyl dextran (CM-dex) and diethylenetriaminepentaacetic acid (DTPA) and reaction schemes for the preparation of ADCs containing these linkers bound to Pt(II) complexes [40–44].

conjugated to CM-dex and the reduction is even higher for the conjugate A5B7-CM-dex-*cis*-DDP. Conjugate A5B7-CM-dex-*cis*-DDP displays the higher half-life. Conjugate A5B7-CM-dex-*cis*-DDP was relatively stable in other tissues (with the exception of the liver). It also had a smaller distribution of platinum to the tissues when compared to free *cis*-DDP. The mechanism of tissue uptake seemed to be similar for unconjugated and conjugated *cis*-DDP [42].

2.1.2.2. Conjugates containing diethylenetriaminepentaacetic acid (DTPA) as linker. A different ligand used as linker between platinum (II) complexes and antibodies is diethylenetriaminepentaacetic acid (DTPA in Scheme 1) which has been extensively used in nuclear medicine. DTPA can be used as an anhydride which can bind covalently primary amine groups of the protein to form amide bonds and to *cis*-DDP through the carboxylate groups [43,44]. In a report from 1991 by Koch and co-workers, the authors described the coupling of *cis*-DDP to purified monoclonal antibodies of different immunoglobulin isotypes IgG1, IgG2, and IgG2b (CD7 T-cell, L-227, S34, 22c6, EBU-141) generating very stable Ig-DTPA-*cis*-DDP conjugates [43]. The mAb employed detected structures on T- or B- lymphocytes and the antibody-drug conjugates (a term used for the first time in a paper involving metal-based drugs) retained the binding affinity towards the lymphocytic cell lines bearing the corresponding antigen [43]. The conjugates were able to specifically inhibit the cell growth of these cell lines (24 h assays with pre-incubation). The conjugates exceeded the antiproliferative effect of *cis*-DDP. While comparing pre-incubation with continuous incubation experiments, the Ig-DTPA-*cis*-DDP conjugates were found as active as *cis*-DPP (a fact to be further considered for potential clinical translation). The authors commented that the antibodies tested (anti T-cell and anti B-cell) were models and explained all the variables necessary for the effectiveness of an antibody drug conjugate [43]. The authors briefly indicated that the use of a different linker (*N*-succinimidyl 3-(2-pyridyldithio)propionate (SPDP) [78]) did not afford stable platinum-containing ADCs.

Beck and co-workers developed antibody drug conjugates between *cis*-DDP and a murine anti-CA125 (anti-ovarian tumor marker) mAb on ovarian cancer cell lines employing the linker DTPA [44]. The conjugate (reported in 1994) [44] was prepared *via* the procedure described by Koch et al. (scheme 1) [43]. As in Koch's report, the immunoconjugates anti-CA125-DTPA-*cis*-DDP were found to maintain the specific biding affinity towards the CA125 antigen but it was found that that the immunoconjugates did not show antiproliferative activity in the NIH:OVCAR 3 ovarian cancer cell lines. The authors provided two different possible explanations: a) that CA125 is released in the cell culture medium in large amounts for this cell and generates soluble immunocomplexes that get “washed away”, and b) that the final concentration (equivalent to 0.5 μM) of cisplatin attached to the Ab may not be sufficient to cause and antiproliferative effect during the 30-min incubation period. The report of Koch et al. [43], described cytotoxic properties with pre-incubation periods of 24 h. Beck and co-workers

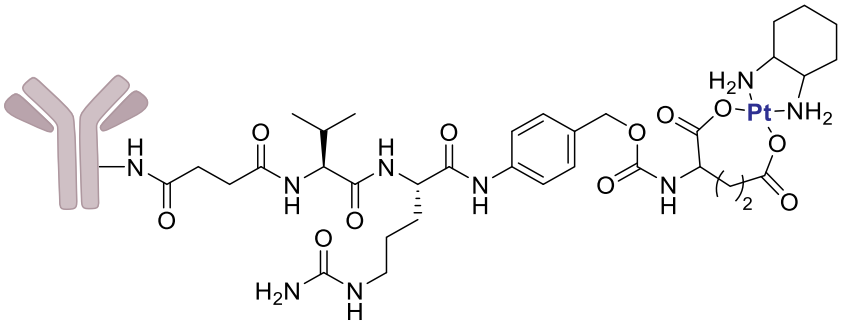

Fig. 3. Schematic structure of Her-Val-Cit-Pt(DACH)(Glu) or Herceptin-Pt(II) [45].

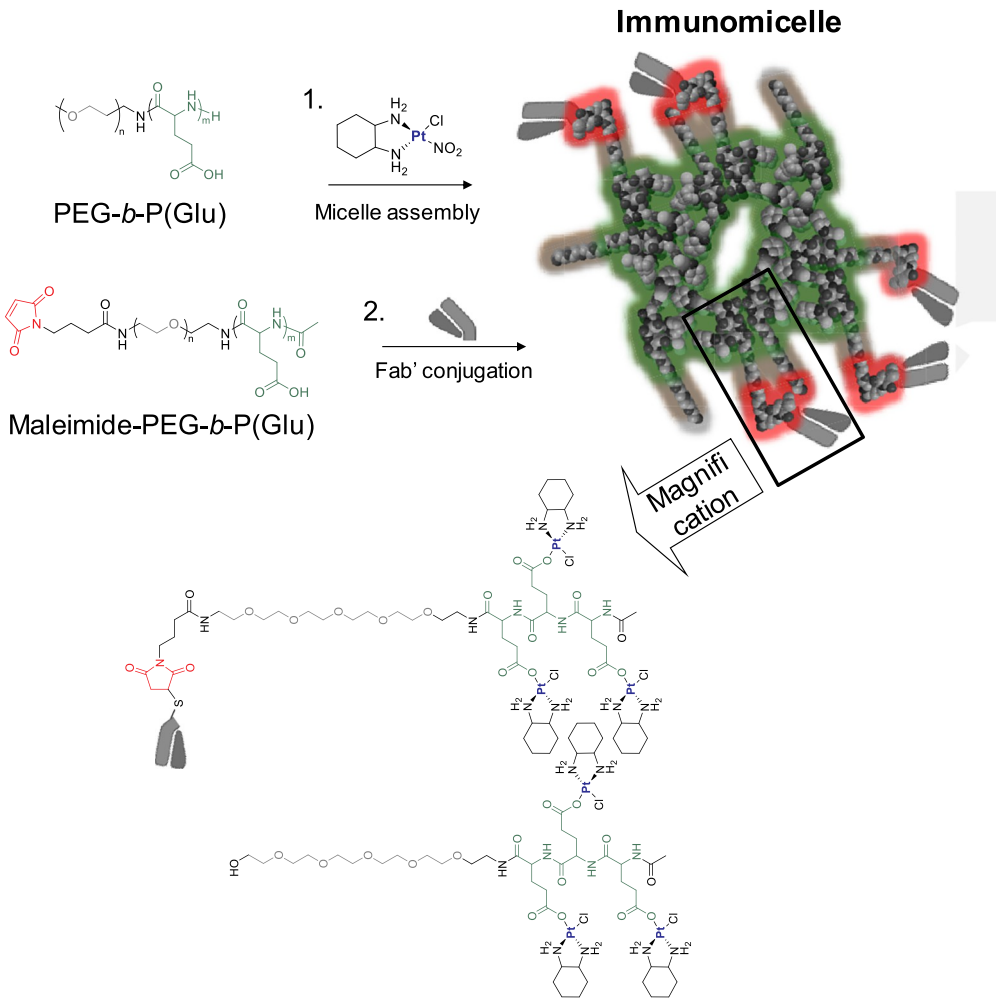

Scheme 2. Preparation of anti-FT Fab′ fragment-installed in polymeric micelles containing a platinum derivative from oxaliplatin (DACHPt/m).

however argued that short pre-incubation periods are a better reflection of the situation *in vivo* [44].

2.1.2.3. Conjugates containing an enzyme-cleavable dipeptide as linker. After these initial reports from the eighties and nineties, research on the topic of platinum-based ADCs was not published until much more recently. In 2015, Zhu and co-workers reported on a platinum(II) containing ADC based on Herceptin, a modified oxaliplatin analogue (Pt(DACH)(Glu) in Fig. 2) and an enzyme-cleavable dipeptide linker based on valine-citrulline (Val-Cit) and a self-immolative spacer (Fig. 3) [45]. The antibody used, humanized IgG1 mAb Herceptin™ from Genentech (also known as Trastuzumab, Tz) has been used either alone, or in combination with chemotherapy, hormone blockers or tyrosine kinase inhibitors for human epidermal growth factor receptor 2 (HER2) positive cancers [79,80]. It has also been used as a delivery vehicle for chemotherapeutics and radioisotopes for the same type of cancers [1,2]. The linker has been used in the lysosomal release of doxorubicin and some other drugs (*e.g.* auristatin) from internalizing immunoconjugates [81]. It is stable in plasma but labile in the presence of Cathepsin B which leads to a 1,6-elimination reaction and activation of drug release. The linker was attached to the Pt(II) compound Pt(DACH)(Glu) through the amine in the side chain (Fig. 2) and the Pt(II)-containing linker was conjugated to Herceptin (Trastuzumab) through the lysine residues (non-specific conjugation). The new Her-Val-Cit-Pt(DACH)(Glu) conjugate (named as Herceptin-Pt(II)) has a DAR (drug to antibody ratio) of 6.4 (as estimated by flameless atomic absorption spectrometry, FAAS).

The authors demonstrated that Herceptin-Pt(II) retains the high and selective binding affinity for HER2 protein (ELISA assay) and HER2-positive SK-BR-3 ovarian cancer cell lines (as assessed by a cellular binding assay using flow cytometry and fluorescence microscopy). In addition, cytotoxicity assays against SK-BR-3 breast cancer cell lines showed that Herceptin-Pt(II) is more cytotoxic than oxaliplatin (19.7 ± 2.2. μM *versus* 31.0 ± 0.1 μM) while not showing growth inhibition on cancer cells (> 50 μM) with a lower or negative HER2 expression (MCF-7 and MDA-MB-231) which corroborates the specificity towards HER2 of the conjugate [45]. While it was found that the combination of Herceptin and oxaliplatin (mixed in a molar ratio similar to the drug to antibody ratio DAR) afforded a similar cytotoxicity (14.4 ± 0.9 μM) it is expected for the conjugates to be specific *in vivo* and that the incorporation of the covalent linkage between the Pt compound and the mAb will decrease the toxicity of the free platinum derivative towards other tissues. Moreover, while compared to free oxaliplatin, the conjugate Herceptin-Pt(II) improved the cellular uptake of the platinum drug in SK-BR-3 cells [45]. However, the cytotoxicity found in the micromolar range for this platform may prevent its potential translation to the clinic.

2.1.3. Platinum compounds encapsulated in carriers bound to mAbs (polymeric micelles, liposomes and protein nanocages)

A possibility to increase the cytotoxic payload of metal-based drugs (like conventional platinum(II) compounds) is to use delivery platforms

(such as nanoparticle-based materials) able to incorporate many more molecules that the classical ADCs and that usually display longer circulation times. Several materials can be envisioned for this purpose such as polymers, liposomes or protein nanocages.

Polymeric micelles have been used for the targeted transport of cancer chemotherapeutics (immunomicelles) [82–86]. These materials can circulate in blood for a longer period of time as their surface is covered by PEG (polyethylene glycol) strands (biocompatible). They also show superior tumor extravasation and penetration, a convenient small size (10 to 100 nm), and a high EPR (enhanced permeability and retention) effect which aids greatly with tumor accumulation. In 2014, Kataoka and co-workers described a platform consisting on polymeric micelles incorporating mAb fragments (anti-tissue factor TF antibody-Fab′ clone 1849) for the targeting and a cytotoxic payload consisting on an active complex of oxaliplatin (DACHPt in Fig. 2) [46]. The platinum compound incorporated in polymeric micelles had been evaluated in clinical trials (phase I) at the time of the report [87] and it was hypothesized that the functionalization of the micelles with the antibody fragments would improve the delivery to the tumors as well as its intracellular release. The incorporation of the platinum compound in the polymeric micelles (to form DACHPt/m) is done *via* coordination of the Pt with the carboxylates of polyglutamic acid (of poly(ethylene glycol)-b-poly(glutamic acid) (PEG-b-P(Glu)) copolymers (Scheme 2). The incorporation of the Fab (fragment antigen binding) in the micelles is done *via* maleimide-thiol conjugation to Mal-DACHPt/m (Scheme 2) [46]. It was observed that one anti-Fab′ was conjugated to each 50% Mal-DACHPt/m and that the content of Pt did not vary by the introduction if the Fab′ (*ca.* 45 Pt/Polymer [wt/wt%]). There was a 15-fold increase in cellular binding activity of the anti-Fab′-DACHPt/m to TF-expressing cells (human pancreatic cancer BxPC-3 cells) as well as very quick cellular internalization. The *in vitro* toxicity on the BxPC-3 cells was determined and it was shown that while DACHPt/m has an IC_{50} of 126 μM, in these cells (48 h incubation time) the anti-TF Fab′-DACHPt/m platform had an IC_{50} of 25 μM similar to that of "free" oxaliplatin (23 μM). As it has been discussed, ADCs are expected to be more advantageous *in vivo* (specifity for tumors and decreased release of cytotoxic drugs to other tissues and organs). The study on mice with subcutaneous BxPC-3 xenografts was performed with free oxaliplatin at 8 mg/kg, and DACHPt/m and anti-Fab′-DACHPt/m (both at 3 mg/kg). The last two platforms showed an enhanced tumor growth inhibition with the anti-Fab′-DACHPt/m suppressing the tumor growth better and for 40 days. Tumor accumulation was similar in both cases indicating that the incorporation of the Fab′ does not improve the tumor accumulation but rather that the improved antitumor effect observed may come from the facilitated cellular uptake *via* TF-targeting.

Based on the same hypothesis of improving targeted delivery, and efficacy of drugs encapsulated in nanocarriers by their functionalization with antibody vectors, Garrido and co-workers reported on the surface functionalization of liposomes (LP) containing oxaliplatin with the mAb Cetuximab CTX (targeting EGFR) or a fragment CTX-Fab′ [47]. Liposome encapsulation is known to improve tumor accumulation (due to their small size and surface PEGylation) as well as to increase blood circulation and decrease drug toxicity and volume of distribution of the drug encapsulated. Immunoliposomes had already been described [88]. The authors used as targeting vector an antibody fragment (smaller than mAb) to eliminate the unwanted immune activity that would come from linking a whole mAb to the liposomal surface (due to the random orientation). Garrido and co-workers studied the platforms in which they linked the mAb CTX for comparison as well [47]. Fig. 4 shows a schematic representation of the two platforms used: CTX-LP-L-OH and CTX-Fab′-LP-L-OH. The functionalization of the liposomes with mAb or mAb-Fab is done *via* maleimide/thiol-ether chemistry. The targeted liposomes are homogeneous (*ca.* 120 nm) and are able to encapsulate as much oxaliplatin L-OH as non-targeted liposomes (ca 32% efficiency of encapsulation and loading capacity of 65.2 ± 7.2 μg/μg lipid). The release of L-OH from non-targeted and targeted liposomes is also similar, up to 25–35% in the first 5 h and then remains constant for 24 h. Presence of serum increases the release in 10–20% (initial phase).

The selective binding of targeted liposomes to overexpressed EGFR in colorectal (CRC) cell lines was demonstrated [47]. The binding was stronger for the LP-CTX-Fab′ than for LP-CTX (although both bind much more strongly than non-targeted liposomes). The cytotoxicity towards all tested EGFR receptor-positive colorectal cancer cell lines of the targeted L-OH liposomes improves with respect to free L-OH and non-targeted liposomal L-OH. Studies *in vivo* in SW-480 colon cancer bearing mice (CRC xenograft model) showed that drug delivery and tumor accumulation was improved significantly for the two targeted platforms described and more especially for the platform containing targeted LP-CTX-Fab′ with respect to non-targeted liposomes containing oxaliplatin or the free drug itself. The efficacy studies showed that while L-OH encapsulated is in general more efficacious than free drug to delay tumor growth, for the platform CTX-Fab′-LP-L-OH this delay was even more pronounced. None of these platforms showed any significant pathological toxicity for the dose of L-OH used [47].

Protein nanocages [89] have also been used quite recently to generate ADCs and they show significant advantages due to: a) their interior can be used for encapsulation or binding of drugs, and b) the exterior surface can be functionalized to incorporate diverse molecules like mAbs. A relevant protein nanocage is ferritin (HFt) [90]. As a natural component of cells and blood, ferritin will be less likely to elicit strong antibody and/or T cell immune responses and is amenable to genetic and chemical modifications.

In 2013 the group of Ceci and co-workers developed an ADC platform based on ferritin conjugated to the mAb Ep1 (anti-CSPG4 antigen) which encapsulates *cis*-DDP (Fig. 5) [48]. The conjugate HFt-Pt-Ep1 is able to encapsulate about 50 *cis*-DDP molecules and has an estimated molecular size of about 900 kD and 33 nm. The ADC retains the specificity to bind CSPG4 + melanoma cell lines but is not specific to

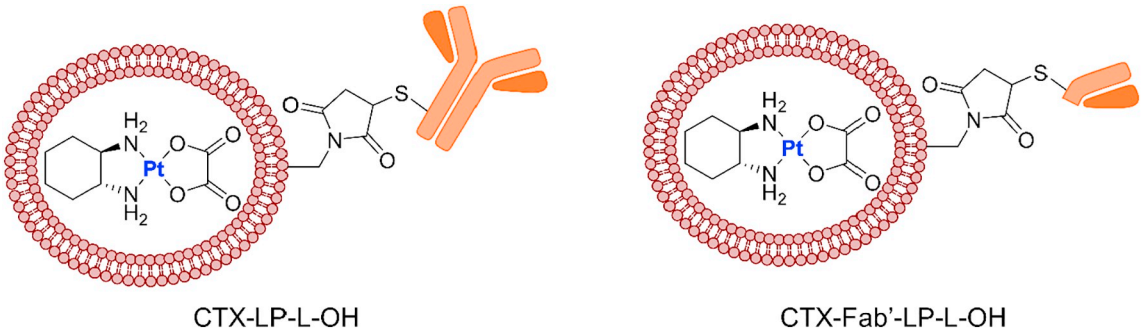

Fig. 4. Schematic representation of ACD platforms consisting on CTX and CTX-Fab′ functionalized liposomes containing oxaliplatin (L-OH): CTX-LP-L-OH and CTX-Fab′-LP-L-OH [47].

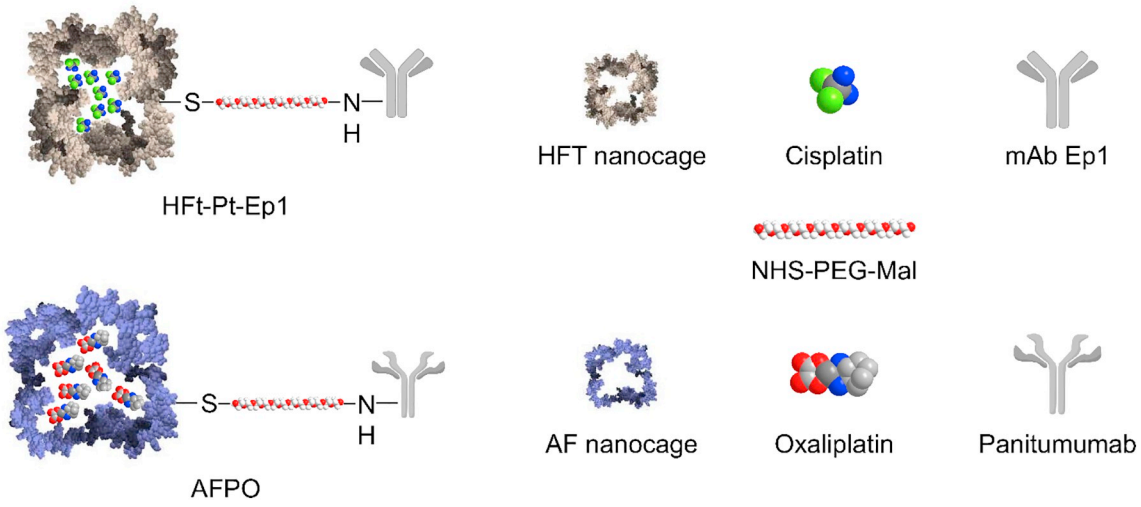

Fig. 5. Structures of ADCs based on protein nanocages functionalized with mAb containing platinum compounds [48,49].

CSPG4- breast carcinoma cell lines. This specificity was demonstrated *in vitro*. Free *cis*-DDP, HFt-Pt and HFt-Pt-Ep1 were tested on melanoma and breast cancer carcinoma expressing or lacking CSPG4 respectively. The ADC conjugate demonstrated an effectivity like *cis*-DDP for melanoma and a 25-fold preference for melanoma cancer cell lines as well [48]. This preference or specificity was also demonstrated *in vivo*. Hft-Pt-Ep1 was able to delay the growth on melanoma xenografts on nude mice whereas growth of tumors in mice with implanted breast carcinoma xenografts was affected to a lesser extent (5-fold) [46]. The authors indicated that the next step will be to humanize the mAb Ep1 *via* recombinant DNA manipulation to be able to minimize the human anti mouse antibody (HAMA) responses [48].

By a similar approach, Shieh and co-workers developed in 2018 a platform based on apoferritin (AF) nanocages linked to mAB panitumumab *via* polyethylene glycol (PEG) linkers that were used to encapsulate oxaliplatin (platform designed as AFPO in Fig. 5) [49]. Panitumumab can specifically target cell lines expressing epidermal growth factor receptor (EGFR). An additional advantage of AF is its pH-sensitive bioreactive cavity. The ADC platform AFPO was studied *in vitro* on colorectal cells expressing EGFR and it was demonstrated that the AFPO is taken up by these cells *via* endocytosis and that it can inhibit cell viability (48 h). AFPO is stable in serum and they incorporated 2 panitumumab molecules on average. In addition, pH-dependent studies showed stability of AFPO over time (no release of free oxaliplatin at pH 7.4) but a release at pH 5. Moreover, *in vivo* studies showed AFPO having a much greater efficacy in mice bearing HCT-116 tumors (high EGFR expression) than the non-targeted AF in which oxaliplatin had been encapsulated (AFO) [49].

The results described in these four reports are extremely promising and demonstrate that immunonanocarriers can indeed increase the therapeutic translational potential of ADCs containing platinum compounds.

2.2. ADCs containing gold payloads

Gold nanoparticles have been used as components of ADCs due to their photodynamic or photothermal properties [52–61], as chemosensitizers [63,64], and as carriers of other cytotoxic payloads [65,66] (to be described in Section 3). ADCs containing discrete gold compounds as cytotoxic payloads have however not been described until 2018 [50,51]. Both reports are based on ADCs containing the anti-HER2 humanized IgG1 mAb Trastuzumab Tz (or an engineered version) and on their efficacy *in vitro* on breast cancer cell lines overexpressing HER2. As mentioned before, Trastuzumab (Herceptin™ from Genentech) has been used in the treatment of HER2 positive cancers [79,80],

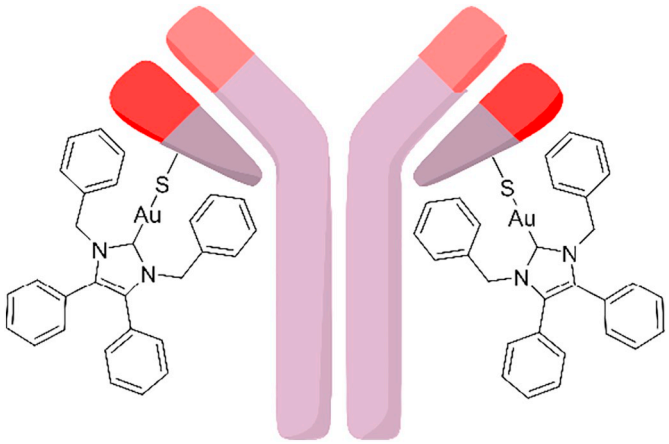

Fig. 6. Schematic representation of Th—Au [51].

and as delivery vehicle for chemotherapeutics and radioisotopes for the same type of cancers [1,2].

The group of Bernardes in collaboration with the group of Tacke, reported on the synthesis of a gold-based ADC containing an engineered Trastuzumab which presents and additional free cysteine per light chain (ThiomAb LC-V205C or Th) [50]. The gold(I) *N*-heterocyclic carbene-containing organometallic compound (Fig. 6) was directly conjugated to the mAb light chain through the thiol from the cysteine groups generating a gold-sulfur bond (conjugate Th—Au in Fig. 6) [50].

This conjugate (obtained with > 95% conversion) was characterized by LC-MS (liquid chromatography-mass spectrometry) and by EI-MS (electron ionization –mass spectrometry). The authors demonstrated the selective binding to a single cysteine residue per light chain by the gold starting material. They obtained a drug to antibody ratio (DAR) of 2 and reported on the specificity and binding capacity to the HER2 antigen overexpressed in the SK-BR-3 breast cancer cell line (by flow cytometry). The IC_{50} obtained by Th—Au in this cell line (9.85 μM) was however quite close to that obtained for the triple negative MDA-MB-231 breast cancer cell line (14.48 μM) or the non-malignant MCF10A (13.22 μM) both which do not overexpress the HER2 receptors. In addition, the IC_{50} for the gold(I) starting material [Au(NCH)Cl] was marginally higher in the three lines studied (13.64 μM for SK-BR-3 breast cancer, 17.69 μM for triple negative MDA-MB-231 breast cancer, and 16.35 μM for the non-malignant MCF 10A) [50]. Ideally the resulting conjugates should have a higher specificity for the

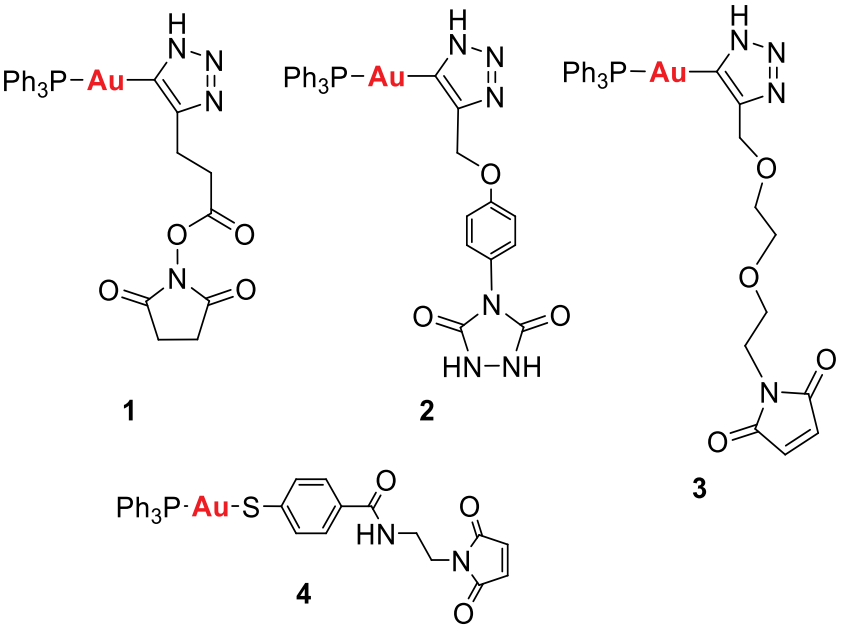

Fig. 7. Linkers containing gold(I) compounds (**1–4**) amenable for bioconjugation with mAb. Adapted from Scheme 1 in ref. [51].

cell lines overexpressing HER2 and a much lower IC_{50} value (nano or sub-nano molar range) as described in the Introduction. In addition, the direct conjugation of the gold atom to the free cysteine of Thiomab in Th—Au may cause a decreased stability *in vivo*.

Our group at Brooklyn College (in collaboration with the group of Lewis at Memorial Sloan Kettering Cancer Center) reported on the same year on Trastuzumab-gold conjugates [51]. We described gold(I)-compounds amenable to bioconjugation *via* ester or maleimide linkers. Fig. 7 depicts the four gold-containing linkers obtained (**1–4**) *via* reaction of commercially available linkers containing a terminal alkyne and $[AuN_3(PPh_3)]$ (**1–3**) (copper-free cycloaddition) or by amide formation between a linker containing a terminal amine and a gold thiolate compound containing a terminal carboxylate group (**4**). These linkers were fully characterized and two (**1** and **4**) were chosen for bioconjugation with Trastuzumab.

Compound **1** activated *N*-Hydroxysuccinimide NHS-ester moiety can react with the cysteine residues of Tz to generate **Tras-1**. For compound **4** a more selective conjugation can take place as its maleimide moiety can react with the Tz cysteine residues after reduction of Tz interchain disulfide bonds to generate **Tras-4** (Scheme 3) [51]. The

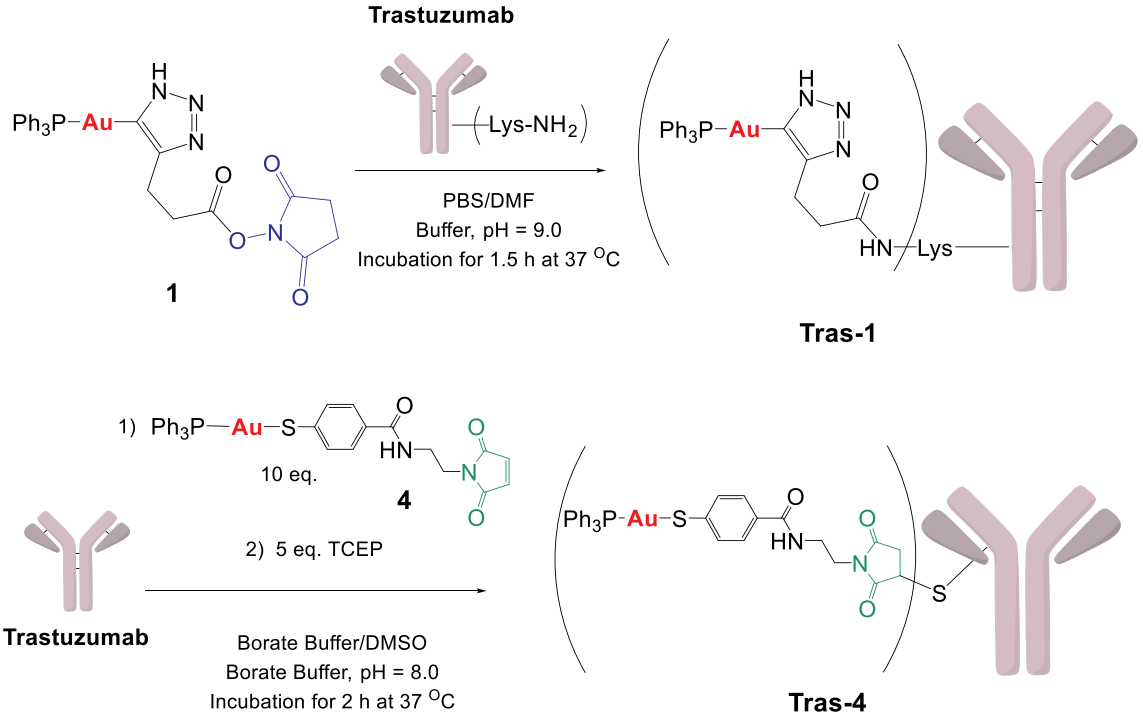

Scheme 3. Preparation of Trastuzumab-gold comjugates **Tras-1** and **Tras-4**. Reproduced from Ref. [51] with permission from the Royal Society of Chemistry.

Table 1
Cell viability EC_{50} values (μM) in breast cancer HER2-positive MCF-7 and BT-474 cells, and non-cancerous breast MCF-10A cells for: a) gold starting materials **[AuCl(PPh_3)]** and **[Au(mba)(PPh_3)]**, b) new gold-containing linkers **1**, and **4**, and c) novel antibody gold-based conjugates **Tras-1** and **Tras-4**. Auranofin (**AF**) was used as control.
Reproduced from Ref. [51] with permission from the Royal Society of Chemistry[a].

	[AuCl(PPh_3)]	[Au(mba)(PPh_3)]	1	4	Tras	Tras-1	Tras-4	AF
MCF-7 (**A**)	3.57 ± 0.33	2.36 ± 0.32	38.76 ± 4.85	2.73 ± 0.86	>60μM	2.67 ± 0.70	0.63 ± 0.05	4.09 ± 0.07
BT-474 (**B**)	3.32 ± 0.10	3.51 ± 0.16	23.28 ± 0.31	0.81 ± 0.01	>60μM	1.73 ± 0.17	0.32 ± 0.01	3.94 ± 0.33
MCF-10A (**C**)	18.94 ± 1.30	5.52 ± 0.36	44.57 ± 5.15	6.77 ± 0.67	>50μM	5.69 ± 0.45	4.04 ± 0.20	3.19 ± 0.45
EC_{50}(**C**)/EC_{50}(**A**)	5.30 ± 0.61	2.34 ± 0.35	1.15 ± 0.20	2.48 ± 0.82	0.83 ± 0.13	2.13 ± 0.58	6.41 ± 0.60	0.78 ± 0.11
EC_{50}(**C**)/EC_{50} (**B**)	5.70 ± 0.43	1.57 ± 0.13	1.91 ± 0.22	8.35 ± 0.83	0.83 ± 0.13	3.29 ± 0.41	12.63 ± 0.74	0.81 ± 0.13

[a] Compounds were dissolved in 1% of DMSO, DMF or DMSO/triethylene glycol (as described in Ref. [51]) and diluted with media before addition to cell culture medium for a 72 hour incubation period. Trastuzumab, **Tras-1** and **Tras-4** were directly diluted in media. Compounds performed in duplicate and STDEV is derived from these two separate experiments.

new antibody gold-conjugates (AGCs) were obtained with yields of 55% and 70% respectively and a purity of > 95% and were characterized by MALDI-TOF and size exclusion HPLC. **Tras-1** resulted in a DAR of 2.7–3.2 and **Tras-4** in a DAR of 2.7 (we had aimed for DARs comprised between 2 and 4). ELISA assays for binding affinity for HER2 showed a slight decreased binding affinity for HER2 for **Tras-1** and **Tras-4** in comparison with Tz. Moreover, we studied the stability of these new conjugates in human serum over a period of 7 days. The presence of unconjugated gold was evaluated by ICP-OES and no release of gold was observed in this period confirming the stability of **Tras-1** and **Tras-4** [51].

The cytotoxicity of the conjugates on HER2 positive breast cancer cells (MCF-7 and BT-474) and on a non-cancerous human breast cell line (MCF-10A) was studied and compared to that of gold starting materials, gold linkers (**1**–**4**) and unmodified Tz (Table 1). The AGCs **Tras-1** and **Tras-4** displayed enhanced cytotoxicity (very low micromolar and sub-micromolar range) compared to the gold linkers (**1** and **4**), or Tz in the HER2 positive cell lines. **Tras-4** was significantly more cytotoxic (10 fold) than starting material [Au(mba)(PPh_3)] in the BT-474 cell line (Table 1). The selectivity of **Tras-4** is also higher compared to conjugate **Tras-1**, all gold starting materials and Auranofin (used as control) [51].

The results of our study were very promising as we had used a non-optimized payload (fragment $[Au(PPh_3)^+]$) and obtained EC_{50} values for the first time in the sub-micromolar range for metal-based ADCs. The use of other gold-cytotoxic payloads (like specific gold-*N*-heterocyclic carbenes) already known to have EC_{50} in the nanomolar range, will undoubtedly help increase the clinical translation potential of gold-based ADCs [51].

Table 2 summarizes the section of ADCs containing metal-based cytotoxic payloads providing a quick visualization in terms of cytotoxic payload, linkers or nanocarriers employed, mAb and cancer cell lines targeted and indicating if *in vivo* studies were performed.

3. ACDs containing metal-based components (nanoparticles) in their structure

Nanoparticles have been used for over two decades in biomedical sciences and engineering. The FDA approved Doxil® (liposomal-encapsulated doxorubicin) in 1995 to avoid cardiomyopathy in long-term treated patients. Nowadays, metal nanoparticles are of interest due to their unique physicochemical properties compared to the bulk material [91]. The most studied metal nanoparticles are those based on silver and gold [92,93].

Gold-nanoparticle (AuNP) properties allow for several applications such as catalysis, electronics, photodynamic therapy, or agent delivery [91]. In addition to these applications, AuNPs can be modified with diverse functional groups which can be conjugated to drugs and/or antibodies to afford nanoADCs [52–66]. NanoADCs have been used in phototherapy (PDT [52–54], photothermal therapy PTT [55–61]) and as chemo-sensitizers [63,64] and as carriers for payloads [65,66] (Fig. 8).

3.1. ADCs containing metallic nanoparticles for phototherapy

Phototherapy is a type of therapy that uses specific light wavelengths of light to irradiate cancerous tissues [94–96]. This type of therapy includes photodynamic therapy (PDT) [97] and photothermal therapy (PTT) (Fig. 8.A) [98]. PDT involves a photosensitizer and a specific light wavelength (from visible to near red). Upon irradiation, the photosensitizer produces singlet oxygen ($^1O_2$) which induces apoptosis through reactive oxygen species (ROS). PTT increases cell temperature after excitation by light absorption that leads to cell death. This process of light-induced temperature elevation is known as hyperthermia. Other variants of PTT use radio frequency, microwaves, air-plasma, or near-infrared region (NIR) instead visible light as hyperthermia agents [97].

3.1.1. Metal nanoparticle-ADCs in photodynamic therapy

Pérez-García and co-workers reported in 2017 on functionalized AuNPs with a tetraphenylporphyrin photosensitizer (PR) and PEG that were conjugated to anti-ErbB2 [52]. PR-AuNP-PEG-Ab conjugate was tested in SK-BR-3 breast cancer cells in the absence and presence of light. Only after irradiation, the cellular morphology changed and there was cell membrane damage [52]. De la Rosa and co-workers developed similar NPs-based platforms [53]. They synthetized $NaYF_4$:Yb,Er up-conversion nanoparticles (UCNPs) covalently bound to a porphyrin-based photosensitizer (ZnPc) conjugated to trastuzumab (Tz). UCNPs can convert NIR light into red light which can subsequently excite ZnPc [53]. HER2-positive and -negative breast-cancer cell lines (SK-BR-3 and MCF-7, respectively) were treated with UCNPs-ZnPC-Tz with and without irradiation. The viability of SK-BR-3 cells was dramatically decreased after irradiation indicating selectivity [53].

Cui and co-workers studied the PTT effect of a cell-based nanoADC *in vitro* and *in vivo*. Gold nanoclusters were assembled using Chlorin e6 (a porphyrin-based photosensitizer) to produce stable nanoparticles which were conjugated to anti-CD3 [54]. Cell-based nanoADC was generated after CIK (Cytokine-induced killer) uptake of Ce6-GNCs-Ab NPs. CIK viability of cell-based nanoADC was not affected in the absence of laser irradiation [54]. Human gastric cancer MGC-803 cells were exposed to Ce6-GNCs-Ab-CIK and CIK cells in the presence or absence of laser irradiation showing that MGC-803 viability was only reduced after Ce6-GNCs-Ab-CIK treatment and irradiation. In addition, *in vivo* studies demonstrated that irradiated cell-based nanoADC displayed a decrease in tumor volume respect to other irradiated treatments [54].

3.1.2. Metal nanoparticle-ADCs in photothermal therapy

The first two examples of ADC-nanoparticles for PTT were published in 2005 [55,56]. Drezek and co-workers reported that nanoshells

Table 2
Summary of ADCs based on metal-containing cytotoxic payloads. Structures of payloads in Figs. 2, 6 and 7. Structures of linkers or carriers in Figs. 3–5 and Schemes 2 and 3.

Metal-based payload	Linker or nanocarrier	mAb or mAb-Fab′	Cells targeted *in vitro*	*In vivo* efficacy studies	*In vivo* PK studies	Toxicity	Selectivity	Ref
K_2PtCl_4 or *cis*-DPP	None	- Anti-YAC Ig - Goat anti-38C-13Ig - Mouse anti-YAC monoclonal Ig	- YAC (Moloney-induced virus lymphoma) - 38C-13 (B-cell leukemia)	No	No	3- to 1.25-fold higher cytotoxicity of Pt-anti-YAC respect to anti-YAC	Pt-anti-YAC is 3-fold more selective than Pt-anti-38 to 38C13 cells	[37]
cis-DDP or *cis*-aq	CM-dex	Goat anti-38C-13	38C-13 (murine model for B-Lymphoma)	No	No	**GI_{50} of Cis-DDP-CM-dex-g-anti-38C-13** 5 μM	Cis-DDP-CM-dex-g-anti-38C-13 is 24-fold more selective than cis-DDP-CM-dex-g-anti-RIgC to 38C13 cells	[40]
cis-DDP	CM-dex	A5B7	LS174T (colorectal carcinoma)	LS174T tumor-bearing nude mice	No Yes	ID_{50} (24 h) 3 μM	A5B7-Dextran Cisplatin more cytotoxic than CM-dextran-Cisplatin	[41,42]
cis-DDP	DTPA	CD7 T-cell - L-227 - S34 - 22c6 - EBU-141	T- or B-lymphocytes	No	No	Inhibition of proliferation of all conjugates at 0.75 mg/L [*cis*-DDP] about 50% in corresponding targeted cells (free cis-DPP 12–24%) when pre-incubated and similar IP at continuous incubation (24 h)	Specific IgG AB conjugates more cytotoxic than cis-DDP *ca.* 2-fold (with pre-incubation) and same cytotoxicity at 24 h incubation	[43]
cis-DDP	DTPA	Anti-CA125	NIH:OVCAR 3 (ovarian cancer)	No	No	No antiproliferative activity on target cell lines (0.5 mg/mL [cis-DPP])	N/A	[44]
cis-DDP	Ferritin (HFt) Nanocage	Ep1	CSPG4 + melanoma	CSPG4 + melanoma xenografts-bearing nude mice	No	Tumor size was reduced 1.2-fold in breast carcinoma and 3.8-fold in melanoma	HFt-Pt-Ep1 is 25-fold more selective to melanoma than breast carcinoma	[48]
MIDP	None	1C1	MCF-7 (breast cancer)	No	Yes	Inhibition of proliferation of all conjugates at 0.63 μg/L [Pt] 50% in corresponding targeted cells (free MDPI 50% at 0.16 μg/L [Pt])	N/A (non-targeted and non-specific conjugates)	[38,39]
Oxaplatin O-LH	Liposomes	Cetuximab CTX or CTX-Fab′ (anti-EGFR)	EFGR + CCR cell lines (colorectal cancer)	SW-480 colon xenografts-bearing mice	Yes	**IC_{50} (μM) of LP-Fab′** 17.19 ± 1.12 (HCT116) 23.82 ± 0.89 (HT29) 28.12 ± 0.40 (SW480) 35.86 ± 3.51 (SW620)	Targeted liposomal L-OH outperformed liposomal and free L-OH in all EGFR overexpressing cell lines (1.5–3-fold)	[47]
Oxaplatin analogue Pt(DACH) (Glu)	(Val-Cit) cleavable dipeptide	Trastuzumab Tz or Herceptin (anti-HER2)	SK-BR-3 MCF-7 (breast cancer)	No	No	**IC_{50} of Tz-Pt(II) (μM)** 19. ± 2.2 (SKBR3) > 50 (MCF7) > 50 (MDAMB231)	Over 2–3 fold more selective to HER2-positive SKBR-3 cell line	[45]
Oxaplatin L-OH	Apoferritin (AF) Nanocage	PanitunumAb (anti-EGFR)	HCT-116 (colorectal)	HCT-116 colorectal xenografts-bearing nude mice	No	Tumor growth inhibition respect control was 2.6-fold in low-expressing EGFR-bearing SW-620 mice and 8.8-fold in high-expressing EGFR-bearing HCT-116 mice	AFPO is 3.4-fold more selective to higher-expressing EGFR than low-expressing EGFR tumors	[49]

(*continued on next page*)

Table 2 (*continued*)

Metal-based payload	Linker or nanocarrier	mAb or mAb-Fab′	Cells targeted *in vitro*	*In vivo* efficacy studies	*In vivo* PK studies	Toxicity	Selectivity	Ref
Oxaplatin analogue DACHPt	Micelles	Anti-tissue factor TF antibody-Fab′ clone 1849	BxPC-3 (pancreatic cancer)	BxPC-3 pancreatic cancer xenografts-bearing mice	No	**IC_{50} (μM) in BxPC3** 23 (oxaliplatin) 126 (DACHPt/m) 25 (anti-TF Fab′-DACHPt/m) N/A (anti-TF Fab′)	N/A	[46]
[AuCl(NHC)]	None	Thiomab LC-V205C Th (anti-HER2)	SKBR3 (breast cancer)	No	No	**GI_{50} (μM)** 9.85 (SKBR3) 14.46 (MDAMB231) 13.32 (MCF10A)	$\frac{GI50(MCF10A)}{GI50(SKBR3)}$ = 1.35 $\frac{GI50(MCF10A)}{GI50(MDAMB231)}$ = 0.92	[50]
[AuCl(PPh_3)]	Commercially available linkers containing a terminal alkyne or amine (Fig. 7)	Trastuzumab Tz or Herceptin (anti-HER2)	MCF-7 BT-474 (breast cancer)	No	No	**EC_{50} of Tras-1 (μM)** 2.67 ± 0.7 (MCF7) 1.73 ± 0.17 (BT474) **EC_{50} of Tras-4 (μM)** 0.63 ± 0.05 (MCF7) 0.32 ± 0.01 (BT474)	$\frac{EC50(MCF10A)}{EC50(MCF7)}$ = 2.13 ± 0.58 (tras-1) 6.41 ± 0.6 (tras-4) $\frac{EC50(MCF10A)}{EC50(BT474)}$ = 3.29 ± 0.41 (Tras-1) 12.63 ± 0.74 (Tras-4)	[51]

(120 nm of silica core NPs covered by 10 nm of gold shell) conjugated to anti-HER2 antibody induced apoptosis in SK-BR-3 breast cancer cell lines [55]. Anti-HER2-nanoshells-treated cells died after exposition to NIH irradiation while no cytotoxicity was found in the absence of irradiation [55]. Not long after Drezek's report, El-Sayed and co-workers published a PTT study using anti-EGFR-AuNPs in three different cell lines [56]. Results showed that the benign epithelial HaCaT cell line presented photothermal destruction at higher irradiance than squamous carcinoma cell lines (HSC 313 and HOC 3 Clone 8) [56]. In 2017, Yang and co-workers conjugated anti-c-Met (hepatocyte growth factor receptor) to hollow gold nanospheres (HGNs) to study the effect of radiotherapy in the human cervical CaSki cell line. CaSki proliferation was only inhibited after X-ray radiation in ADC-nanospheres-treated-cells [57].

Gold nanorods (GNRs) can also be used in PTT due to their characteristic surface plasmon resonance (SPR) effect [99]. He and co-workers studied the application of anti-EGFR-GNRs for *in vitro* and *in vivo* PTT [58]. Anti-EGFR-GNRs were not cytotoxic in Hep-2 or in human bronchial epithelial cell line Beas-2B in darkness. However, anti-EGFR-GNRs inhibited growth of human laryngeal epithelioma Hep-2 cells at low irradiance. In addition, *in vivo* studies showed that anti-EGFR-GNR after irradiation, significantly inhibited tumor growth of Hep-2 xenografts with an effect comparable to that of cisplatin [58]. Years later, Zhang's group reported on *in vitro* and *in vivo* studies of gold nanorods-porphyrin-trastuzumab (TGNs) complexes [59]. In short, HER2-positive breast cancer cells (BT-474 and SK-BR-3) underwent apoptosis after TGNs treatment and irradiation. The viability of non-cancerous human breast cell line MCF-10A was not affected indicating Ab specificity. Similarly, the tumor volume in xenografted mice models was dramatically reduced post-treatment with TGN and laser irradiation [59].

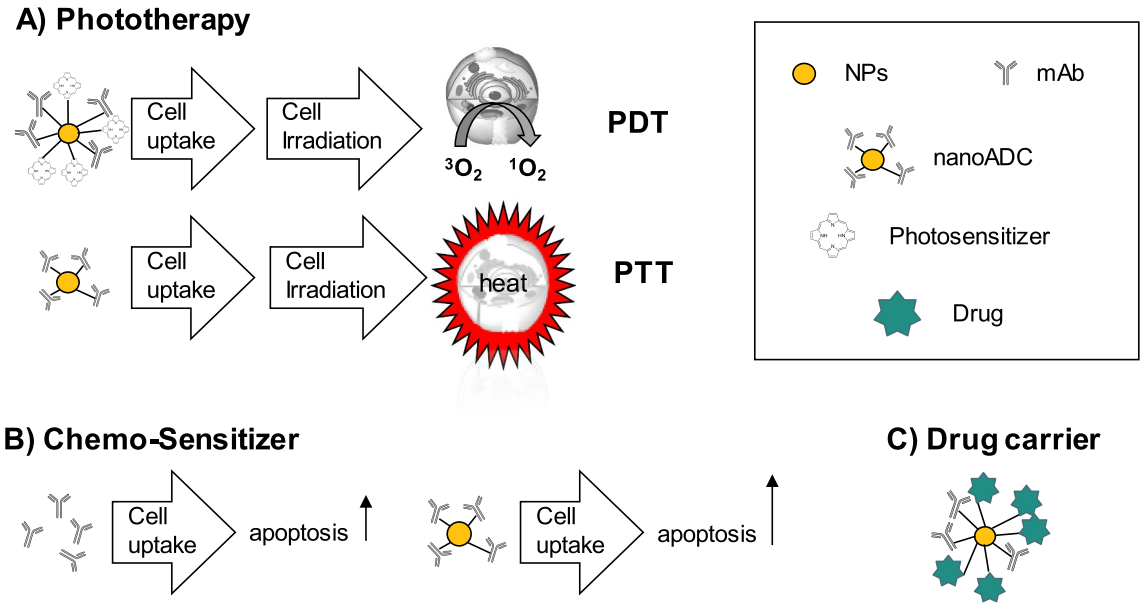

Fig. 8. Different applications of gold nanoADCs [52–66].

3.1.3. Nanoparticle-ADCs as hyperthermia agents.

Although there have been a larger number of reports on PTT, other nanoADCs that use sources other than visible light to induce hyperthermia have been reported. For example, in 2008 Lee and co-workers prepared AuNP conjugated to anti-phospho-FAK to study the effect of air-plasma irradiation and gold nanoparticle ADCs in melanoma cells [60]. The authors treated G361 human melanoma cells with AuNP and p-FAK-AuNP in the dark and did not observe cytotoxicity. Remarkably, plasma irradiation in combination with AuNP and p-FAK-AuNP exposure, increased cell death dramatically [60]. Years later, Kim and co-workers reported that p-FAK-AuNP presented cytotoxicity in G361 cells but not in HaCaT (immortalized human keratinocyte) normal cells indicating specificity due to the Ab [61]. Moreover, cell death rates were 3-fold higher in G361 than in HaCaT cells after p-FAK-AuNP treatment followed by plasma irradiation [61].

3.2. ADCs containing metallic nanoparticle's which act as chemo-sensitizers or carriers for other drug payloads

A number of reports stated that AuNPs do not present toxic effect unless the NP diameter is below 3 nm [100,101]. However, several examples are now known for which gold nanoparticles (d > 3 nm) bound to mAbs exhibit cytotoxicity [63,64]. These cytotoxic effects have been used to develop AuNPs-based ADCs for two different purposes. Gold nanoparticles can sensitize cancerous cells to the effects of chemotherapy (Fig. 8.B.) [63,64] or can be used as carriers of cytotoxic payloads to target cancer cells after antibody conjugation (Fig. 8.C.) [65,66].

In addition to the uses of AuNPs in therapeutic applications, they can also be utilized to study the colloidal stability and aggregation level of the AuNPs-Ab platforms in different freeze-drying formulation (by evaluation of metal content and antibody efficiency) [62].

3.2.1. ADCs containing gold nanoparticles which act as chemosensitizers

Xu and Yin in 2014 reported that CTX-AuNP inhibited cell proliferation and migration while triggering CTX-induced apoptosis *in vitro* [63]. Antibody properties were not impaired; A549 cell line exhibited a statistically significant response to CTX while H1299 cells did not (high- and low-EGFR expression, respectively). In addition, *in vivo* analysis showed significant tumor growth decrease in A549 xenografted mice supporting the results obtained *in vitro* [63]. One year later, Pelaz, Rejman and co-workers successfully conjugated AuNPs to anti-VEGF (vascular endothelial growth factor) and anti-HRP (horseradish peroxidase) antibodies without inducing agglomeration. Unfortunately, Au-PEG-anti-VEGF and Au-PEG-anti-HRP NPs exhibited similar cell viability values which indicates antibody deactivation [64].

3.2.2. ADCs containing gold nanoparticles which act as carriers for cytotoxic payloads

The first example of AuNPs bound to mAbs as carriers was reported by Basu and co-workers in 2011 [65]. Briefly, AuNPs were incubated with the VEGFR (vascular endothelial growth factor receptor) antibody and subsequently with doxorubicin. Bovine aortic endothelial BAEC cells were treated with Au-anti-VEGFR-2-doxorubicin nanobioconjugate showing that the mechanism of uptake is through endocytosis. Additionally, cargo delivery specificity was demonstrated by treatment of negative control NIH3T3 (mouse embryonic fibroblast) cells and by receptor competition assay [65]. Years later, Shapter and co-workers reported Paclitaxel-Gold nanoparticles (PTX-AuNPs) conjugated to either TARP or EpCAM antibodies [66]. These AuNPs-based platforms were tested *in vitro* in T-47D (human breast cancer cell) cells demonstrating that PTX-AuNPs-Ab presented a higher cytotoxicity than either Ab-AuNPs or PTX-AuNPs. From the two antibodies tested, TARP exhibited higher cytotoxic effect than EpCAM against T-47D cell line [66].

4. ACDs containing metal-based components (single molecules) in their structure

As mentioned in the Introduction, linkers are a critical component for the successful translation of ADCs to the clinic [1–10]. Linkers already described are mostly built by organic molecules but some metal-linkers based on ethylenediamine platinum (II) complexes (*Lx*) have also been reported (Fig. 9) [67–70].

The group of van Dongen reported in 2015 the coupling of 4-nitrobenzo-2-oxa-1,3-diazole (NBD) fluorophore to Trastuzumab (Tz) using ethylenediamine platinum (II) as linker (Fig. 9.A.) [67]. NBD was tethered to the linker through ligands such as *N*-coordinated amines (heteroaromatic and aliphatic) or *S*-coordinated thioethers [67]. Further studies of this group focused on *in vitro* and *in vivo* analysis [68,69] of *Lx*-based ADCs such as Trastuzumab-coupled to ^{89}Zr-labeled Desferal and Trastuzumab-coupled to Auristatin F. Biodistribution studies showed that ADC conjugates were stable and therefore further antibody modifications were not deemed necessary [68,69]. In addition, the *Lx*-linker (as part of the ADC) did not afford side reactions after *in vivo* administration. An increase in the cytotoxic effect of Auristatin F-ADC was demonstrated [68].

In 2016 Roy, Sengupta and co-workers attached PEG-Camptothecin (PEG-CPT) to Trastuzumab (Tz), Cetuximab (CTX), and Rituximab (RTX) by reaction of the *Lx*-linker with the disulfide bridges from the antibody (Fig. 9.B) [70]. The DAR values obtained were ~8 and the linker generated did not compromise the antibody properties or ADC stability. This *Lx*-ADC was more stable than maleimide-ADC and exhibited higher cytotoxicity [70].

5. Conclusions and outlook

In conclusion, we have demonstrated that while the field of ADCs has burgeoned in the past thirty plus years, metal-based ADCs have been overlooked. We only found about twenty examples (fifteen reports) of ADCs containing metal-based cytotoxic payloads (based on platinum and gold) from which only a few were properly characterized. This is therefore a research area with enormous potential, but scientists have to take into consideration all advances already made in ADC research and technology over the years. In this regard, the optimal selection of antibodies (humanized) and of site-specific and stable linkers, and very importantly the judicious choice of metal-based payload is crucial for any potential translation to the clinic. From the studies reported in this review it is clear that only highly or extremely highly cytotoxic metal compounds should be employed for their conjugation to antibodies to generate classical ADCs with any translational potential. ADCs based on traditional platinum compounds do not have the cytotoxicity necessary for successful clinical development. There are however other metals like gold able to afford highly cytotoxic compounds that should be further explored. Another area worth of mention is the use of antibody fragments (nanobodies) instead of antibodies. These are single-domain antibody fragments (mostly based on naturally heavy chain variable domains) that are usually a tenth of the size of mAb. Researchers will have to pay considerable attention to the stability of new bioconjugates in human plasma before proceeding with more advanced preclinical studies. In this review we also highlight recent advances in nanotechnology that have provided antibody-modified nanocarriers as excellent targeted delivery vehicles for metal-based payloads. These inmuno-nanocarriers are usually biocompatible and stable and allow for the incorporation of a higher number of cytotoxic drugs per platform unit and an improved pharmacological profile. We anticipate many advances in this field. The review has also covered the utilization of metal-based nanoparticles with different applications (such as PTD and PTT therapy, as chemosensitizers and nanocarriers of pay-loads) that can target tumors by bioconjugation to mAB. This seems to be unquestionably an emerging field. Lastly, the utilization of platinum-based compounds in the structure of linkers for the development

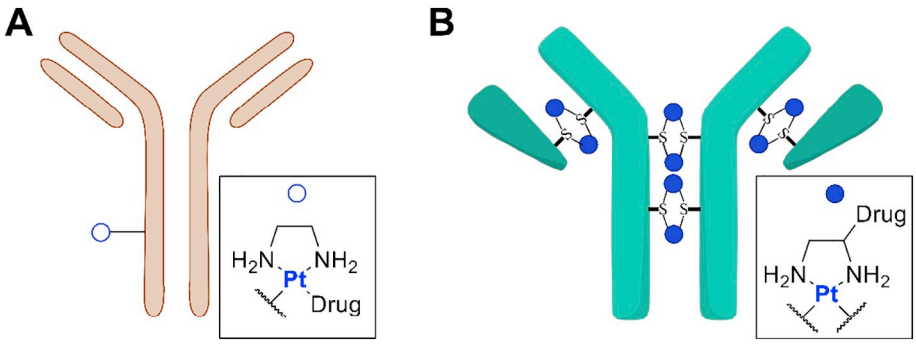

Fig. 9. Simplified representation of ADCs using different Pt-linkers.

of ADCs has become a novel strategy to dramatically increase the stability of the linkers. To conclude, we anticipate a number of contributions from the inorganic medicinal chemistry community which will advance the exciting field of ADCs in the near future.

Abbreviations

Ab	Antibody
anti-c-Met	hepatocyte growth factor receptor
ADC	Antibody Drug Conjugate
AGC	Antibody Gold Conjugate
AF	Apoferritin
anti-CA125	anti-ovarian tumor marker
ARC	Antibody Radionucleide Conjugate
AuNP	Gold nanoparticle
CEA	carcinoembryonic antigen
Ce6	Chlorin e6 (porphiryn photosensitizer)
CIK	Cytokine-induced killer cells
Cis-DDP	*cis*-platin
CPT	Camptothecin
CRC	colorectal
CTX	Cetuximab
DACH	1,2-diamminocyclohexane
DTPA	Diethylenetriaminepentaacetic Acid
DAR	Drug to Antibody Ratio
EDC/NHS	1-Ethyl-3-(3-dimethylaminopropyl)carbodiimide/*N*-Hydroxysuccinimide
EGFR	Epidermal Growth Factor Receptor
EPR	Enhanced Permeability and Retention
ESI-MS	Electrospray Ionization-Mass Spectrometry
FAAS	Flameless Atomic Absorption Spectrometry
Fab	fragment antigen binding
GNRs	Gold Nano Rods
HAMA	Human Anti Mouse Antibody
Hep-2	human laryngeal epithelioma
HER-2	human epidermal growth factor receptor 2
HGNs	Hollow Gold Nanospheres
HPLC	High Performance Liquid Chromatography
HRP	horseradish peroxidase
HSA	Human Serum Albumin
HFt	Ferritin
Ig	Immunoglobulin
LC-MS	Liquid Chromatography-Mass Spectrometry
L-OH	oxaliplatin
LP	Liposome
Lx	Ethylenediamine platinum (II) complex
mAb	Monoclonal Antibody
mAb-Fab'	Monoclonal Antibody Fragment
MALDI-MS	Matrix-Assisted Laser Desorption/Ionization Mass Spectrometry
MIDP	Methyliminodiacetato-*trans*-*R*,*R*-1,2-diamminocyclohexane
NBD	4-nitrobenzo-2-oxa-1,3-diazole
NHS	*N*-Hydroxysuccinimide
NIR	Near-Infrared Region
PDT	Photodynamic Therapy
PEG	Polyethylene Glycol
PR	tetraphenylporphyrin photosensitizer
PTT	Photothermal Therapy
PTX	Paclitaxel
ROS	reactive oxygen species
RTX	Rituximab
SATP	*N*-succinimidyl-*S*-acetylthiopropionate
SPDP	*N*-succinimidyl 3-(2-pyridyldithio)propionate
SPR	Surface Plasmon Resonance
TGNs	Gold nanorods-porphyrin-trastuzumab
Tz	Trastuzumab or Herceptin (humanized IgG1 mAb Herceptin™ from Genentech)
VEGF	vascular endothelial growth factor
VEGFR	vascular endothelial growth factor receptor
UCNPs	Up-conversion nanoparticles
ZnPc	Zinc tetracarboxyphenoxy phthalocyanine

Declaration of Competing Interest

None.

Acknowledgment

This work was supported by National Institutes of Health (NIH) grant 2SC1GM127278-05A1 (M.C.).

References

[1] L. Ducry, B. Stump, Bioconjug. Chem. 21 (2010) 5–13.
[2] Antibody-drug conjugates, in: L. Ducry (Ed.), Methods in Molecular Biology, 1045 Springer Protocols, Humana Press, 2014.
[3] A. Thomas, B.A. Teicher, R. Hassan, Lancet Oncol 17 (2016) e254–e262.
[4] P. Polakis, Pharmacol. Rev. 68 (2016) 3–19.
[5] B.E.C.G. de Goeij, J.M. Lambert, Curr. Opin. Inmunol. 40 (2016) 14–23.
[6] N. Diamantis, U. Banerji, Brit. J. Cancer 114 (2016) 362–367.
[7] L.N. Turney, Med. Chem. Rev. 52 (2017) 363–381.
[8] J.M. Lambert, A. Berkenblit, Annu. Rev. Med. 69 (2018) 191–207.
[9] P.J. Carter, G.A. Lazar, Nat. Rev. 17 (2018) 197–223.
[10] T. Rodrigues, G.J.L. Bernardes, Angew. Chem. Int. Ed. 57 (2018) 2032–2034.
[11] H. Kaplon, J.M. Reichert, MAbs 11 (2019) 219–238.
[12] https://adcreview.com/news/adc-market-reach-us-3-billion-2018.
[13] J.M. Lambert, Curr. Opin. Pharmacol. 5 (2005) 543–549.
[14] C. Chalouni, S. Doll, J. Exp. Clin. Cancer Res. 37 (20) (2018) 2–12.
[15] A.H. Stadaucher, M.P. Brown, Brit. J. Cancer. 117 (2017) 1736–1742.
[16] S. García-Alonso, A. Ocaña, A. Pandiella, Cancer Res. 78 (2018) 2159–2165.
[17] G. Casi, D. Neri, Mol. Pharm. 12 (2015) 1880–1884.
[18] J. Lu, F. Jiang, A. Lu, G, Int. J. Mol. Sci. (2016) 17:561.
[19] S. Panowski, S. Bhakta, H. Raab, P. Polakis, J.R. Junutula, MAbs 6 (2014) 34–45.
[20] P. Agarwal, C.R. Bertozzi, Bioconjug. Chem. 26 (2015) 176–192.
[21] D. Schumacher, C.P.R. Hackenberger, H. Leonhardt, J. Helma, J. Clin. Immunol. 36 (2016) S100–S107.
[22] D. Sussman, L. Westendorf, D.W. Meyer, C.I. Leiske, M. Anderson, N.M. Okeley,

S.C. Alley, R. Lyon, R.J. Anderson, P.J. Carter, D.R. Benjamin, Protein Eng. Des. Sel. 31 (2017) 47–54.
[23] A. Casini, A. Vessières, S.M. Meier-Menches (Eds.), Metal-based Anticancer Agents, Book Series Metallobiology, Royal Society of Chemistry, 2019.
[24] B. Engliner, C. Pirker, P. Heffeter, A. Terenzi, C.R. Kowol, B.K. Keppler, W. Berger, Chem. Rev. 119 (2019) 1519–1624.
[25] S. Monro, K.L. Colon, H. Yin, J. Roque, P. Konda, S. Gujar, R.P. Thummel, L. Lilge, C.G. Cameron, S.A. McFarland, Chem. Rev. 119 (2019) 797–828.
[26] Metallo-drugs: development and action of anticancer agents, in: A. Sigel, H. Sigel, E. Freisinger, R.K.O. Sigel (Eds.), Metal Ions in Life Sciences, 18 Walter de Gruyter, Berlin, Germany, 2018.
[27] A.T. Chan, M.M. Hsu, B.C. Goh, E.P. Hui, T.W. Liu, M.J. Millward, R.L. Hong, J. Whang-Peng, B.B. Ma, K.F. To, M. Mueser, N. Amellal, X. Lin, A.Y. Chang, J. Clin. Oncol. 23 (2005) 3568–3576.
[28] J.B. Vermorken, R. Mesia, F. Rivera, E. Remenar, A. Kawecki, S. Rottey, J. Erfan, D. Zabolotnyy, H.R. Kienzer, D. Cupissol, F. Peyrade, M. Benasso, I. Vynnychenko, D. De Raucourt, C. Bokemeyer, A. Schueler, N. Amellal, R. Hitt, N. Engl. J. Med. 359 (2008) 1116–1127.
[29] Y. Kurokawa, N. Sugimoto, H. Miwa, M. Tsuda, S. Nishina, H. Okuda, H. Imamura, M. Gamoh, D. Sakai, T. Shimokawa, Y. Komatsu, Y. Doki, T. Tsujinaka, H. Furukawa, Brit. J. Cancer 110 (2014) 1163–1168.
[30] K.N. Moore, D.M. O'malley, I. Vergote, L.P. Martin, A. Gonzalez-Martin, K. Malek, M.J. Birrer, Gynecol. Oncol. 151 (2018) 46–52.
[31] R.J. Pietras, B.M. Fendly, V.R. Chazin, M.D. Pegram, S.B. Howell, D.J. Slamon, Oncogene 9 (1994) 1829–1838.
[32] D. Balin-Gauthier, J.P. Delord, M.J. Pillaire, P. Rochaix, J.S. Hoffman, R. Bugat, C. Cazaux, P. Canal, B.C. Allal, Brit. J. Cancer 98 (2008) 120–128.
[33] C. Oliveras-Ferraros, A. Vazquez-Martin, E. Lopez-Bonet, B. Martin-Castillo, S. Del Barco, J. Brunet, J.A. Menendez, Int. J. Oncol. 33 (2008) 1165–1176.
[34] A. Gornowicz, A. Bielawska, R. Czarnomysy, H. Gabryel-Porowska, A. Muszynska, K. Bielawski, Mol. Cell. Biochem. 408 (2015) 103–113.
[35] S. Saha, X.M. Zhang, D. Dimitrov, Z. Zhu, B.S. Croix, E. Zudaire, Combination Therapies Using Platinum Agents and TEM8 Monoclonal Antibodies for Target Tumor-associated Stroma or Tumor Cells, WO2015191596A1 (2015).
[36] A. Gornowicz, A. Bielawska, W. Szymanowski, H. Gabryel-Porowska, R. Czarnomysy, K. Bielawski, Oncol. Lett. 15 (2018) 2340–2348.
[37] E. Hurwitz, R. Kashi, M. Wilchek, J. Natl. Cancer Inst. 69 (1982) 47–51.
[38] M.G. Rosenblum, J.L. Murray, S. Stuckey, R.A. Newman, S. Chaney, A.R. Khokhar, Cancer Chemother. Pharmacol. 25 (1990) 405–410.
[39] M.G. Rosenblum, J.L. Murray, P.J. Kelleher, R.A. Newman, A.R. Khokhar, Monoclonal Antibodies Binding Platinum Complexes, US5053226A, (1991).
[40] B. Schechter, R. Puazner, R. Arnon, J. Haimovich, M. Wilcheck, Cancer Immunol. Immunother. 25 (1987) 225–230.
[41] D.P. McIntosh, R.J. Cooke, L.A. Gilford, M. Rowland, P.T. Daley-Yates, Antibody, Immunoconjugates, and Radiopharmaceuticals 7 (1994) 117–131.
[42] D.P. McIntosh, R.J. Cooke, A.J. McLachlan, P.T. Daley-Yates, M. Rowland, J. Pharm. Sci. 86 (1997) 1478–1483.
[43] B. Koch, W. Baum, E. Beck, G. Eger, P. Rohwer, J.R. Kalden, M. Gramatzki, Antibody, Immunoconjugates, and Radiopharmaceuticals 4 (1991) 121–132.
[44] E. Bec, M. Hoffmann, G. Bernhardt, W. Jager, L. Wildt, N. Lang, Cell Biophys.. 24/25 (1994) 163–173.
[45] R. Huang, Y. Sun, X.Y. Zhang, B.W. Sun, Q.C. Wang, J. Zhu, Biomed. Pharmacother. 73 (2015) 116–122.
[46] J. Ahn, Y. Miura, N. Yamada, T. Chida, X. Liu, A. Kim, R. Sato, R. Tsumura, Y. Koga, M. Yasunaga, N. Nishiyama, Y. Matsumura, H. Cabral, K. Kataoka, Biomaterials 39 (2015) 23–30.
[47] S. Zalba, A.M. Contreras, A. Haeri, T.L. Ten Hagen, I. Navarro, G. Koning, M.J. Garrido, J. Control. Release 210 (2015) 26–38.
[48] E. Falvo, E. Tremante, R. Fraioli, C. Leonetti, C. Zamparelli, A. Boffi, V. Morea, P. Ceci, P. Giacomini, Nanoscale 5 (2013) 12278–12285.
[49] C.Y. Lin, S.J. Yang, C.L. Peng, M.J. Shieh, ACS Appl. Mater. Interfaces 10 (2018) 6096–6106.
[50] M.J. Matos, C. Labão-Almeida, D. Sayers, O. Dada, M. Tacke, G.J.L. Bernardes, Chem. Eur. J. 24 (2018) 12250–12253.
[51] N. Curado, G. Dewaele-Le Roi, S. Poty, J.S. Lewis, M. Contel, Chem. Comm. 55 (2019) 1394–1397.
[52] O. Penon, M.J. Marin, D.A. Russell, L. Perez-Garcia, J. Colloid Interf. Sci. 496 (2017) 100–110.
[53] G. Ramírez-García, S.S. Panikar, T. López-Luke, V. Piazza, M.A. Honorato-Colin, T. Camacho-Villegas, R. Hernández-Gutiérrez, E. De la Rosa, Nanoscale 10 (2018) 10154–10165.
[54] F. Xia, W. Hou, Y. Liu, W. Wang, Y. Han, M. Yang, X. Zhi, C. Li, D. Qi, T. Li, J. Martinez De La Fuente, C. Zhang, J. Song, D. Cui, Biomaterials 170 (2018) 1–11.
[55] C. Loo, A. Lowery, N. Halas, J. West, R. Drezek, Nanolett 5 (2005) 709–711.
[56] I.H. El-Sayed, X. Huang, M. El-Sayed, Cancer Lett. 239 (2006) 129–135.
[57] Y. Liang, J. Liu, T. Liu, X. Yang, Mater. Lett. 14 (2017) 2254–2260.
[58] S. Zhang, Y. Li, X. He, S. Dong, Y. Huang, X. Li, Y. Li, C. Jin, Y. Zhang, Y. Wang, Int. J. Nanomedicine 9 (2014) 1931–1946.
[59] X. Kang, X. Guo, X. Niu, W. An, S. Li, Z. Liu, Y. Yang, N. Wang, Q. Jiang, C. Yan, H. Wang, Q. Zhang, Sci. Rep. 7 (2017) 42069.
[60] G.C. Kim, G.J. Kim, S.R. Park, S.M. Jeon, H.J. Seo, F. Iza, J.K. Lee, J. Phys. D. Appl. Phys. 42 (2009) 032005(5 pp).
[61] B.B.R. Choi, J.H. Choi, J.W. Hong, K.W. Song, H.J. Lee, U.K. Kim, G.C. Kim, Int. J. Med. Sci. 14 (2017) 1101–1109.
[62] M.A. Hamaly, S.R. Abulateefeh, K.M. Al-Qaoud, A.M. Alkilany, Int. J. Pharm. 550 (2018) 269–277.
[63] Y. Qian, M. Qiu, Q. Wu, Y. Tian, Y. Zhang, N. Gu, S. Li, L. Xu, R. Yin, Sci. Rep. 4 (2014) 7490.
[64] G. Tan, K. Kantner, Q. Zhang, M.G. Soliman, P. Del Pino, W.J. Parak, M.A. Onur, D. Valdeperez, J. Rejman, B. Pelaz, Nanomaterials 5 (2015) 1297–1316.
[65] A. Das, E. Soehnlen, S. Woods, R. Hegde, A. Henry, A. Gericke, S. Basu, J. Nanopart. Res. 13 (2011) 6283–6290.
[66] Z. Alhalili, J. Shapter, D. Figueroa, B. Sanderson, Drug Delivery Lett 8 (2018) 217–225.
[67] D.C. Waalboer, J.A. Muns, N.J. Sijbrandi, R.B. Schasfoort, R. Haselberg, G.W. Somsen, H.J. Houthoff, G.A. Van Dongen, ChemMedChem 10 (2015) 797–803.
[68] N.J. Sijbrandi, E. Merkul, J.A. Muns, D.C. Waalboer, K. Adamzek, M. Bolijn, V. Montserrat, G.W. Somsen, R. Haselberg, P.J. Steverink, H.J. Houthoff, G.A. van Dongen, Cancer Res. 77 (2017) 257–267.
[69] J.A. Muns, V. Montserrat, H.J. Houthoff, K. Codée-van der Schilden, O. Zwaagstra, N.J. Sijbrandi, E. Merkul, G.A.M.S. van Dongen, J. Nucl. Med. 59 (2018) 1146–1151.
[70] N. Gupta, J. Kancharla, S. Kaushik, A. Ansari, S. Hossain, R. Goyal, M. Pandey, J. Sivaccumar, S. Hussain, A. Sarkar, A. Sengupta, S.K. Mandal, M. Roy, S. Sengupta, Chem. Sci. 8 (2017) 2387–2395.
[71] L.M. Carter, S. Poty, S.K. Sharma, J.S. Lewis, J. Label. Compd. Radiopharm. 61 (2018) 611–635.
[72] J.S. Kim, Nucl. Med. Mol. Imaging 50 (2016) 104–111.
[73] K.L. Moek, D. Giesen, I.C. Kok, D.J.A. de Groot, M. Jalving, R.S.N. Fehrmann, M.N. Lub-de Hooge, A.H. Brouwers, E.G.E. de Vries, J. Nucl. Med. (2017) 83S–90S.
[74] R.M. Colman, J. Diesenhofer, R. Huber, W. Palm, J. Mol. Biol. 100 (1976) 257–282.
[75] B. Schechter, R. Pauzner, M. Wilchek, R. Arnon, Cancer Biochem. Biophys. 8 (1986) 289–298.
[76] B. Schecter, R. Pauzner, R. Arnon, M. Wilchek, Cancer Biochem. Biophys. 8 (1986) 277–287.
[77] B. Schecter, M. Wilchek, R. Arnon, Int. J. Cancer 39 (1987) 409–413.
[78] J. Carlson, H. Drevin, R. Axen, Biochem. J. 173 (1978) 723–737.
[79] J. Mendelsohn, J. Baselga, Semin. Oncol. 33 (2006) 369–385.
[80] J. Baselga, S.M. Swain, Nature Rev. Cancer 9 (2009) 463–475.
[81] S.C. Jeffrey, M.Y. Torgov, J.B. Andreyka, L. Boddington, C.C. Cerveny, W.A. Denny, K.A. Gordon, D. Gustin, J. Huagen, T. Kline, M.T. Nguyen, P.D. Senter, J. Med. Chem. 48 (2005) 1344–1358.
[82] Z. Gao, A.N. Lukyanov, A.R. Chakilam, V.P. Torchillin, J. Drug Target. 11 (2003) 87–92.
[83] V.P. Torchillin, A.N. Lukyanov, Z. Gao, B. Papahadjopoulos-Sternberg, Proc. Natl. Acd. Sci. USA 100 (2003) 6039–6044.
[84] T. Noh, Y.H. Kook, C. Park, H. Youn, H. Kim, E.T. Oh, E.K. Choi, H.J. Park, C. Kim, J. Polym. Sci. Pol. Chem. 46 (2008) 7321–7331.
[85] W. Li, H. Zhao, W. Quian, H. Li, L. Zhang, Z. Ye, G. Zhang, M. Xia, J. Li, J. Gao, G. Kou, J. Dai, H. Wang, Y. Guo, Biomaterials 33 (2012) 5349–5362.
[86] H. Song, R. He, K. Wang, J. Ruan, C. Bao, N. Li, J. Ji, D. Cui, Biomaterials 31 (2010) 2302–2312.
[87] H. Cabral, K. Kataoka, J. Control. Release 190 (2014) 465–476.
[88] S. Song, D. Liu, J. Peng, Y. Sun, Z. Li, J.R. Gu, Y. Xu, Int. J. Pharma. 363 (2008) 155–161.
[89] S.A. Bode, I.J. Minten, R.J. Nolte, J.J. Cornelissen, Nanoscale 3 (2011) 2376–2389.
[90] E. Valero, S. Tambalo, P. Mazorla, M. Ortega-Munoz, F.J. Lopez-Jaramillo, F. Santoyo-Gonzalez, J.D. Lopez, J.J. Delgado, J.J. Calvino, R. Cuesta, J.M. Dominguez-Vera, N. Galvez, J. Am. Chem. Soc. 133 (2011) 4889–4895.
[91] K. Mahato, S. Nagpal, M.A. Shah, A. Srivastava, P.K. Maurya, S. Roy, A. Jaiswal, R. Singh, P. Chandra, 3 Biotech 9 (2019) 57.
[92] M. Yamada, M. Foote, T.W. Prow, Wiley Interdiscip. Rev. Nanomed. Nanobiotechnol. 7 (2015) 428–445.
[93] P. Malik, T.K. Mukherjee, Int. J. Pharm. 553 (2018) 483–509.
[94] L. Cheng, C. Wang, L. Feng, K. Yang, Z. Liu, Chem. Rev. 114 (2014) 10869–10939.
[95] P. Błaszkiewicz, M. Kotkowiak, Curr. Med. Chem. 25 (2018) 5914–5929.
[96] H. Kim, K. Chung, S. Lee, D.H. Kim, H. Lee, Wiley Interdiscip. Rev. Nanomed. Nanobiotechnol. 8 (2016) 23–45.
[97] A.M. Rkein, D.M. Ozog, Dermatol. Clin. 32 (2014) 415–425.
[98] S.M. Amini, J. Therm. Biol. 79 (2019) 81–84.
[99] N. Elahi, M. Kamali, M.H. Baghersad, Talanta 184 (2018) 537–556.
[100] A.M. Alkilany, C.J. Murphy, J. Nanopart. Res. 12 (2010) 2313–2333.
[101] G. Schmid, W.G. Kreyling, U. Simon, Arch. Toxicol. 91 (2017) 3011–3037.